Feshbach Resonances in Ultracold Gases

Sara L. Campbell
MIT Department of Physics
(Dated: May 15, 2009)

First described by Herman Feshbach in a 1958 paper, Feshbach resonances describe resonant scattering between two particles when their incoming energies are very close to those of a two-particle bound state. Feshbach resonances were first applied to tune the interactions between ultracold Fermi gases in the late 1990's. Here, we review two simple models of a Feshbach resonance: a spherical well model and a coupled square well model. coupled square well model of a Feshbach resonance and explain how it can be implemented on cold alkali atoms experimentally. Then, we review some recent key developments in atomic physics that would not have been realized without Feshbach resonances.

1. INTRODUCTION AND HISTORY

In 1958, Hermann Feshbach developed a new unified theory of nuclear reactions[1] to treat nucleon scattering. Feshbach described a situation of resonant scattering that occurs whenever the initial scattering is equal to that of a bound state between the nucleon and the nucleus.[2] In the late 1990's, atomic physicists began to take advantage of the kind of resonant scattering proposed by Feshbach to realize resonant scattering between ultracold alkali atoms. Previously, laser and evaporative cooling of atoms had allowed physicists to reach temperatures as low as 1 μK. However, it is much harder to cool molecules, because their energy levels and structure are much more complicated than those of a single atom. Feshbach resonances made it possible to create ultracold molecules by assembling them from ultracold atoms[2], thus making phenomena such as molecular Bose-Einstein condensation and fermionic superfluidity a reality.

2. ESSENTIAL RESULTS FROM SCATTERING THEORY

In a general scattering problem, we have an incident plane wave with wave number k and a radial scattered wave with anisotropy term $f(\theta)$,[3]

$$\phi_{\text{inc}} = e^{ikz}, \phi_{\text{sc}} = \frac{f(\theta)e^{ikr}}{r}. \tag{1}$$

$$d\sigma = |f(\theta)|^2 d\Omega. \tag{2}$$

So, we see that $|f(\theta)|^2$ relates the amplitude of particles passing through a particular target area to the number of particles passing through a solid angle at a particular angle θ.

Now we consider a particle with mass m, energy $\hbar^2k^2/2m$ in a central potential $V(r)$. We can find $f(\theta)$ by considering the wave function at large r, where it is simply the sum of the incident and scattered waves[4],

$$\phi_{\text{large } r} = \phi_{\text{inc}} + \phi_{\text{sc}} = e^{ikz} + \frac{f(\theta)e^{ikr}}{r} \tag{3}$$

We also express the wave function at large r as the solution to Schrödinger's equation. $V(r)$ is a central potential, so the equation is separable. We use partial wave analysis to express our wave function as the sum of the spherical harmonics Y_l and solutions to Schrödinger's radial equation $R(r)$. We assume symmetry about the angle ϕ, so we ignore the quantum number m. The spherical harmonics then are just proportional to the Legendre polynomicals P_l.[5]

$$\phi_{\text{large r}} = Y(\theta)R(r) \tag{4}$$

$$= \left(\sum_{l=0}^{\infty} C_l P_l(\cos\theta)\right) \frac{1}{kr} \sin\left(kr - \frac{l\pi}{2} + \delta_l\right). \tag{5}$$

We expand the e^{ikz} terms and equate coefficients to obtain[4],

$$f(\theta) = \frac{1}{k}\sum_{l=0}^{\infty} \sin\delta_l P_l(\cos\theta). \tag{6}$$

The different angular momentum quantum numbers l correspond to different partial waves. Recall Schrödinger's radial equation,

$$-\frac{\hbar^2}{2m}\frac{d^2u(r)}{dr^2} + V_{\text{eff}}(r)u(r) = Eu(r), \tag{7}$$

where,

$$V_{\text{eff}}(r) = V(r) + \frac{\hbar^2 l(l+1)}{2mr^2}. \tag{8}$$

For the low particle energies in ultracold atoms[6], if $l > 0$ the angular momentum barrier term in Schrödinger's radial wave equation prevents the particle from reaching small r. Using the assumption that $V(r)$ is only significant for small r, we find that only the $l = 0$ or the s-waves in the expansion interact with the potential. $P_0 = 1$, so

$$\phi_{\text{large r}} = \frac{C_0}{kr}\sin(kr - \delta_0), \tag{9}$$

which implies that,

$$f = -\frac{1}{k}e^{i\delta_0}\sin\delta_0 = \frac{1}{k}\frac{\sin\delta_0}{\cos\delta_0 - i\sin\delta_0} = \frac{1}{k\cot\delta_0 - ik}. \tag{10}$$

By definition, the s-wave scattering length a is[7],

$$a = -\lim_{k\to 0} \frac{\tan\delta_0(k)}{k}. \tag{11}$$

For strong attractive interactions, a is large and negative. For strong repulsive interactions, a is large and positive. Also, Taylor expanding $k\cot(\delta_0(k))$ in k^2 gives[6],

$$k\cot(\delta_0(k)) = -\frac{1}{a} + \frac{1}{2}r_{\text{eff}}k^2 + \cdots, \tag{12}$$

where r_{eff} is the effective range of the potential. Combining equations (10) and (12) gives the following expression for $f(k)$ which will be useful later,

$$f(k) = \frac{1}{-\frac{1}{a} + r_{\text{eff}}\frac{k^2}{2} - ik}. \tag{13}$$

Finally, we quote the Lippmann-Schwinger[8][2] equation, which expresses f in terms of the wavevectors $\mathbf{k} and \mathbf{k}'$ of the two particles and the interatomic potential v,

$$f(\mathbf{k}',\mathbf{k}) = -\frac{v(k'-k)}{4\pi} + \int \frac{d^3q}{(2\pi)^2}\frac{v(\mathbf{k}'-\mathbf{q})f(\mathbf{q},\mathbf{k})}{k^2-q^2+\imath\eta}. \tag{14}$$

For s-waves, $f(\mathbf{q},\mathbf{k}) \approx f(k)$, so we can take f outside the integral and also let $v_0 = v(0$. Then,

$$\frac{1}{f(k)} \approx -\frac{4\pi}{v_0} + \frac{4\pi}{v_0}\int \frac{d^3q}{(2\pi)^3}\frac{v(\mathbf{q})}{k^2-q^2+i\eta}. \tag{15}$$

3. APPLICATION TO ULTRACOLD FERMI GASES

Experimentally, we can take advantage of the internal structure of atoms to tune their interaction. The effective interaction potential of the two fermionic atoms depends the angular momentum coupling of their two valence electrons, $|s_1,m_1\rangle \otimes |s_2,m_2\rangle$, where s is the total spin quantum number and m is the spin projection quantum number. If the valance electrons are in the singlet state with the antisymmetric spin wave function,

$$|0,0\rangle = \frac{1}{\sqrt{2}}(\uparrow\downarrow - \downarrow\uparrow), \tag{16}$$

then they have a symmetric spatial wave function and can exist close together. If the valance electrons are in the triplet state and have one of the following symmetric spin wave functions,

$$|1,1\rangle = \uparrow\uparrow \tag{17}$$

$$|1,0\rangle = \frac{1}{\sqrt{2}}(\uparrow\downarrow + \downarrow\uparrow) \tag{18}$$

$$|1,-1\rangle = \downarrow\downarrow \tag{19}$$

then they have an antisymmetric spatial wave function and cannot exist close together. Therefore, the singlet potential V_s tends to be much deeper than the triplet potential V_T. For simplicity, in both models we assume V_s just deep enough to contain one bound state and that V_T contains no bound states, and $0 < V_{\text{hf}} \ll V_T, V_S, \Delta\mu B$.

In addition to the effective interaction potential, if the nucleus has spin $\mathbf{I}$ and the electron has spin $\mathbf{S}$, there is a hyperfine interaction between the electron spin and the nucleus spin[6],

$$V_{\text{hf}} = \frac{\alpha}{\hbar^2}\mathbf{I}\cdot\mathbf{S}. \tag{20}$$

If we apply an external magnetic field B, then there will also be Zeeman shifting $\Delta\mu B$ between the triplet and singlet states, where $\Delta\mu$ is the difference in magnetic moments betwee the two states.

In the field of ultracold atoms, the gas temperature T is very small and the atoms are confined in space using a magneto-optical trap (MOT) so that the atoms feel a considerable magnetic field B. Therefore, $\Delta\mu \gg k_BT$, and if we assume sufficiently low gas density, we can apply Maxwell-Botzmann statistics to the system and see that almost all of the atoms scatter via the $|\uparrow\uparrow\rangle$ state and very few atoms scatter via the $|\downarrow\downarrow\rangle$ state. Using the language of scattering theory, we call $|\uparrow\uparrow\rangle$ an *open channel* and $|\downarrow\downarrow\rangle$ a *closed channel*.[2]

3.1. Spherical Well Model

In this model we only consider one bound state in the closed channel $|m\rangle$ and a continuum of plane waves of relative momentum $\mathbf{k}$ between the two atoms $|k\rangle$ in the open channel.[10] Without coupling, $|m\rangle$ and $|k\rangle$ are energy eigenstates of the free Hamiltonian[2],

$$H_0|k\rangle = 2\epsilon_k|k\rangle, \epsilon_k = \frac{\hbar^2k^2}{2m} H_0|m\rangle = \delta|m\rangle \tag{21}$$

Let $|\phi\rangle$ be the coupled wavefunction, which can be written as a superposition of the molecular state and the scattering states,

$$|\phi\rangle = \alpha|m\rangle + \sum_k c_k|k\rangle. \tag{22}$$

Figure 1 shows how the bound states couple to the continuum. We will solve for the coupling explicitly by plugging $|\phi\rangle$ into Schrödinger's equation with the Hamiltonian $H = H_0 + V$, where V includes the coupling $\langle m|V|k\rangle = g_k/\sqrt{\Omega}$, where Ω is the phase space volume of the system. Because we are just dealing with s-waves, we make the approximation,

$$g_k = \begin{cases} g_0, & E < E_R \\ 0, & E > E_R \end{cases}, \tag{23}$$

where $E_R = \hbar^2/mR^2$.

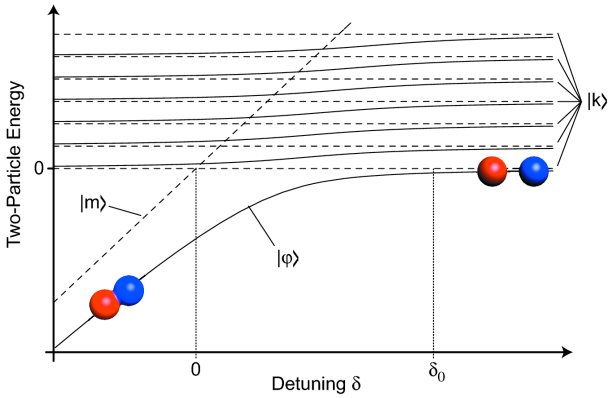

FIG. 1: Energy as a function of detuning for states in the spherical well model for fermion collisions. The uncoupled molecular state $|m\rangle$ and scattering states $|k\rangle$ are shown as dashed lines and the coupled states are shown as solid lines. From [2].

3.1.1. Bound state energy and resonance shift

Then to find the molecular wavefunction after coupling, we plug $|\phi\rangle$ into the time-independent Schrödinger equation $H|\phi\rangle = E|\phi\rangle$ for $E < 0$ and find[2],

$$(E - 2\epsilon)c_0 = \frac{g_0}{\sqrt{\Omega}}\alpha \tag{24}$$

$$(E - \delta)\alpha = \frac{1}{\sqrt{\Omega}} g_0 c_0 = \frac{1}{\Omega}\frac{g_0^2 \alpha}{E - 2\epsilon} \tag{25}$$

$$E - \delta = \frac{1}{\Omega}\sum_k \frac{g_0^2}{E - 2\epsilon}. \tag{26}$$

Integrating over the continuum then gives[2],

$$|E| + \delta = \frac{g_0^2}{\Omega}\int_0^{E_R} \frac{\rho(\epsilon)d\epsilon}{2\epsilon + |E|} \tag{27}$$

$$= \frac{g_0^2 \rho(E_R)}{\Omega}\left[1 - \sqrt{\frac{|E|}{2E_r}}\arctan\left(\sqrt{\frac{2E_R}{|E|}}\right)\right] \tag{28}$$

$$\approx \begin{cases} \delta_0 - \sqrt{2E_0|E|}, & |E| \ll E_R \\ \delta_0\left(\frac{2E_R}{3|E|}\right), & |E| \gg E_R \end{cases} \tag{29}$$

where,

$$\delta_0 = \frac{g_0^2}{\Omega}\sum_k \frac{1}{2\epsilon_k} = \frac{4}{\pi}\sqrt{E_0 E_r}, \tag{30}$$

$$E_0 = \left[\frac{g_0^2}{2\pi}\left(\frac{m}{2\hbar^2}\right)^{3/2}\right]^2. \tag{31}$$

$$E = \begin{cases} -E_0 + \delta - \delta_0 + \sqrt{(E_0 - \delta + \delta_0)^2 - (\delta - \delta_0)^2}, & |E| \ll E_R \\ \frac{delta}{2} - \sqrt{\frac{\delta^2}{4} + \frac{2}{3}\delta_0 E_R}, & |E| \gg E_R \end{cases} \tag{32}$$

As in figure 1, we see that relative to the "bare" $|m\rangle$ state, the "dressed" ground state resonance position is shifted to δ_0.[10]

3.1.2. Scattering amplitude and scattering length

To find the scattering amplitude and scattering length, we plug $|\phi\rangle$ into the time-independent Schrödinger equation $H|\phi\rangle = E|\phi\rangle$ for $E > 0$ and find,

$$(E - 2\epsilon)c_0 = \frac{g_k}{\sqrt{\Omega}}\alpha = \sum_q \frac{g_0}{\sqrt{\Omega}}\frac{1}{E - \delta + i\eta}\frac{g_q}{\sqrt{\Omega}}c_q \tag{33}$$

$$= \sum_q V_{\text{eff}}(k,q)c_q. \tag{34}$$

Substituting $v_0 = V_{\text{eff}}\Omega$ into equation **??** we find,

$$\frac{1}{f_0(k)} \approx \frac{4\pi\hbar^2}{m g_0^2}(E - \delta) + 4\pi\int \frac{d^3q}{(2\pi)^3}\frac{1}{k^2 - q^2 + i\eta}. \tag{35}$$

Now we substitute in,

$$-4\pi\int \frac{d^3q}{(2\pi)^3}\frac{1}{q^2} = \frac{-4\pi\hbar^2\delta_0}{m g_0^2} \tag{36}$$

and also using equation (32) that when $\delta \approx \delta_0$, the energy E is approximately the coupling energy g_0, we find,

$$\frac{1}{f_0(k)} \approx -\sqrt{\frac{m}{2\hbar^2 E_0}(\delta_0 - \delta)} - \frac{1}{2}\sqrt{\frac{2\hbar^2}{m E_0}}k^2 - ik \tag{37}$$

Now our equation looks just like equation (13), so we find a and r_{eff},

$$a = \sqrt{\frac{2\hbar^2 E_0}{m}}\frac{1}{\delta_0 - \delta}, r_{\text{eff}} = -\sqrt{\frac{2\hbar^2}{m E_0}}. \tag{38}$$

Finally, we plug in $\delta - \delta_0 = \Delta\mu(B - B_0)$ to find that,

$$a = -\sqrt{\frac{2\hbar E_0}{m}}\frac{1}{B - B_0}. \tag{39}$$

This is the scattering length we find without considering background collisions in the open channel. We account for background scattering by adding a phase shift δ_{bg} to our wavefunction so that $\delta_{\text{total}} = \delta + \delta_{\text{bg}}$. To see how this extra phase shift affects the scattering length, we add δ_{bg} to our definition of scattering length in equation 11,

$$a_{\text{total}} = \lim_{k\to 0} -\frac{\tan(\delta_0(k) + \delta_{\text{bg}})}{k} \tag{40}$$

$$= \lim_{k\to 0} -\frac{\tan\delta_0(k) + \tan\delta_{bg}}{k(1 - \tan\delta_0\tan\delta_{\text{bg}})} \tag{41}$$

$$\approx \lim_{k\to 0} -\frac{\tan\delta_0}{k} + \lim_{k\to 0}\frac{\tan\delta_{bg}}{k} \tag{42}$$

$$= a + a_{\text{bg}}. \tag{43}$$

So, using this approximation,

$$a_{\text{total}} = a_{\text{bg}} + a = a_{\text{bg}}\left(1 - \frac{\Delta B}{B - B_0}\right), \tag{44}$$

where,

$$\Delta B = \sqrt{\frac{2\hbar^2 E_0}{m}}\frac{1}{\Delta\mu a_{\text{bg}}}. \tag{45}$$

3.2. Coupled Square Well Model

Putting all of these effects together into one Hamiltonian, the Schrödinger equation for a triplet state $|T\rangle$ and a singlet state $|S\rangle$ with potentials $V_T(\mathbf{r})$ and $V_s(\mathbf{r})$ is[4],

$$\begin{pmatrix} \frac{-\hbar^2\nabla^2}{m} + V_T(\mathbf{r}) - E & V_{\text{hf}} \\ V_{\text{hf}} & -\frac{\hbar^2\nabla^2}{m} + \Delta\mu B + V_S(\mathbf{r}) - E \end{pmatrix} \tag{46}$$

$$\times \begin{pmatrix} \psi_{\text{T}}(\mathbf{r}) \\ \psi_{\text{S}}(\mathbf{r}) \end{pmatrix} = 0. \tag{47}$$

As before, we use square well models (for simplicity we use the same radius R) for the two interaction potentials,

$$V_{T,S}(r) = \begin{cases} -V_{T,S}, & r < R \\ 0, & r > R \end{cases} \tag{48}$$

The kinetic energy operator is diagonal because our basis kets are two different internal states of the atoms, so we need to diagonalize the Hamiltonian,

$$H_{\text{int}} = \begin{pmatrix} 0 & V_{\text{hf}} \\ V_{\text{hf}} & \Delta\mu B \end{pmatrix}, \tag{49}$$

and the energy eigenvalues are,

$$E_{\pm} = \frac{\Delta\mu B}{2} \pm \frac{1}{2}\sqrt{(\Delta\mu B)^2 + (2V_{\text{hf}})^2} \tag{50}$$

Let, $Q(\theta)$ be the rotation matrix that diagonalizes the Hamiltonian H and

$$\begin{pmatrix} |\uparrow\uparrow\rangle \\ |\downarrow\downarrow\rangle \end{pmatrix} = Q \begin{pmatrix} |T\rangle \\ |S\rangle \end{pmatrix}. \tag{51}$$

Also, define $V_{\uparrow\uparrow}(\mathbf{r})$, $V_{\uparrow\downarrow}(\mathbf{r})$ and $V_{\downarrow\downarrow}(\mathbf{r})$ by the change of basis formula,

$$\begin{pmatrix} V_{\uparrow\uparrow}(\mathbf{r}) & V_{\uparrow\downarrow}(\mathbf{r}) \\ V_{\uparrow\downarrow}(\mathbf{r}) & V_{\downarrow\downarrow}(\mathbf{r}) \end{pmatrix} = Q(\theta) \begin{pmatrix} V_T(\mathbf{r}) & 0 \\ 0 & V_S(\mathbf{s}) \end{pmatrix} Q^{-1}(\theta). \tag{52}$$

Plugging these new basis states into the Schrödinger equation gives,

$$\begin{pmatrix} -\frac{\hbar^2\nabla^2}{m} + V_{\uparrow\uparrow}(\mathbf{r}) - E & V_{\uparrow\downarrow}(\mathbf{r}) \\ V_{\uparrow\downarrow}(\mathbf{r}) & -\frac{\hbar^2\nabla^2}{m} + E_+ - E_- + V_{\downarrow\downarrow}(\mathbf{r}) - E \end{pmatrix} \tag{53}$$

$$\times \begin{pmatrix} \phi_{\uparrow\uparrow}(\mathbf{r})\phi_{\downarrow\downarrow}(\mathbf{r}) \end{pmatrix} = 0. \tag{54}$$

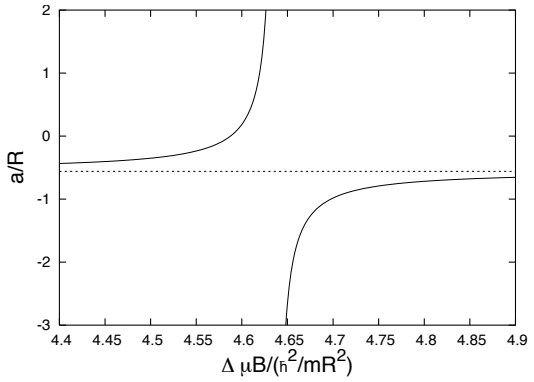

FIG. 2: Theoretical scattering length vs. magnetic field, numerically calculated for the coupled square well model. From [6].

Now we find the s-wave scattering length. Similar to traditional s-wave scattering, for $r > R$ we assume the solutions to the spherical Schrödinger's equation,

$$\begin{pmatrix} u_{\uparrow\uparrow}(r) \\ u_{\downarrow\downarrow}(r) \end{pmatrix} = \begin{pmatrix} Ce^{ikr} + De^{ikr} \\ Fe^{-k'r} \end{pmatrix}, \tag{55}$$

where $k' = \sqrt{m(E_+ - E_-)/\hbar^2 - k^2}$. And for $r < R$ we assume the solutions,

$$\begin{pmatrix} v_{\uparrow\uparrow}(r) \\ v_{\downarrow\downarrow(r)} \end{pmatrix} = \begin{pmatrix} A(e^{ik_1 r} - e^{-ik_1 r}) \\ B(e^{ik_1' r} - e^{-ik_1' r}) \end{pmatrix}, \tag{56}$$

where,

$$k_1 = \sqrt{m(E_- - E_{1,-})/\hbar^2 + k^2} \tag{57}$$

$$k_1' = \sqrt{m(E_- - E_{1,+})/\hbar^2 + k2} \tag{58}$$

$$E_{1,\pm} = \frac{\Delta\mu B - V_T - V_s}{2} \mp \frac{1}{2}\sqrt{(V_s - V_T - \Delta\mu B)^2 + (2V_{\text{hf}})^2}. \tag{59}$$

Finally, $u_{\uparrow\uparrow}$ and $v_{\uparrow\uparrow}$ and their derivatives must match at $r = R$. The same applies to $u_{\downarrow\downarrow}$ and $v_{\downarrow\downarrow}$. The analytical solution is complicated, but a numerical solution of the scattering length a for $V_S = 10\hbar^2/mR^2$, $V_T = \hbar^2/mR^2$ and $V_{\text{hf}} = .1\hbar^2/mR^2$ was calculated as a function of $\Delta\mu B$ and plotted in figure 2, and qualitatively looks very similar to the spherical well solution in equation (44). Both models show the essential physics - that the scattering length is a widely-tunable function of the applied magnetic field.

4. EXPERIMENTAL OBSERVATION OF FESHBACH RESONANCES

4.1. Setup

First predicted for ultracold gases in 1995[11], Feshbach resonances in a Bose-Einstein condensate were

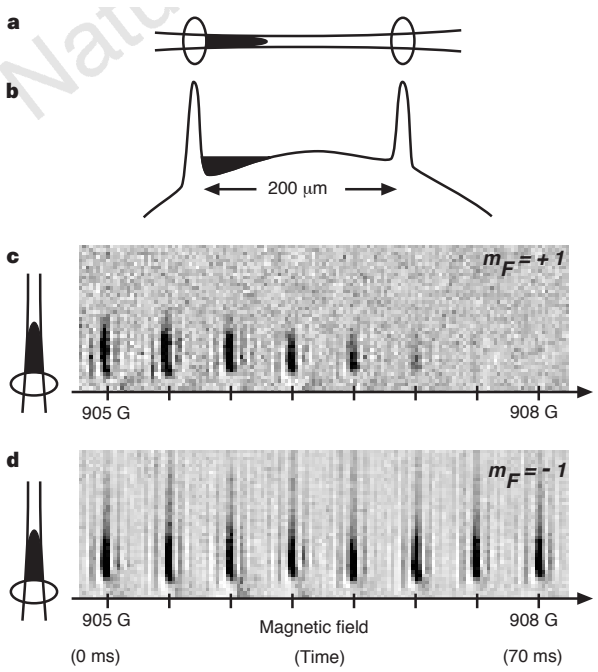

FIG. 3: Illustration of experimental method of phase-contrast imaging in an optical trap. a. Shows the optical trap, made of a red-detuned laser beam for radial confinement and two blue-detuned beams for axial confinement ("endcaps"). b. Shows the confining potential in the axial direction. c and d. show images of the condensate as a function of magnetic field for the $m_F = \pm 1$ substates. From [12]

first observed by the Ketterle group in 1998[12][13]. A schematic of the experimental setup for the 1998 experiment is shown in figure 3. Condensates were prepared in a MOT in the $|F = 1, m_F = -1\rangle$ state, moved to an optical dipole trap (ODT), adiabatically spin-flipped by an RF field to the $|F = 1, m_F = +1\rangle$ state. The condensate was observed using both phase-contrast imaging and time-of-flight absorption imaging[12].

4.2. Finding the resonances

To realize a Feshbach resonance, a large magnetic field was applied to the condensate and swept in magnitude. On one side of a Feshbach resonance, the scattering length is very large and negative, interactions between the atoms are very strong and attractive, and the condensate collapses. On the other side of a Feshbach resonance, the scattering length is very large and positive, interactions between the atoms are very strong and repulsive, and the condensate is quickly lost. The exact locations of the Feshbach resonances in sodium were found by sweeping the magnetic field, finding the magnetic field values with condensate loss, and then sweeping in smaller and smaller intervals about those intervals.[12]. Figure 3c shows condensate loss in the $|F = 1, m_F = +1\rangle$ state as the magnetic field is swept from 905 to 908 G. In figure 4 we also see a sharp drop in the atom number and mean density at the resonance.

4.3. Measuring the scattering length

The interaction energy E_I of the condensate is proportional to the scattering length,[12][14]

$$\frac{E_I}{N} = \frac{2\pi\hbar^2}{m} a\langle n\rangle, \tag{60}$$

where N is the total number of atoms, m is the mass of an atom, and $\langle n\rangle$ is the average density of the condensate. Because the kinetic energy of atoms in a trapped condensate is insignificant compared to the interaction energy, the kinetic energy of a freely expanding condensate defined by the root mean square velocity $v_{\rm rms}$ equals the the interaction energy of the gas while it was trapped,

$$\frac{E_K}{N} = \frac{1}{2} m v_{\rm rms}^2. \tag{61}$$

From [14] we know that,

$$\langle n\rangle \propto N(Na)^{-3/5}. \tag{62}$$

Combining, we find,

$$a \propto \frac{v_{\rm rms}^2}{N}. \tag{63}$$

We can determine both $v_{\rm rms}^2$ and N from time of flight images at a particular magnetic field. This is how we obtain data points for a scattering length vs. magnetic field curve shown in figure 4. The results are very similar to the theoretical model (44)

5. CONCLUSIONS

We have discussed the theory of Feshbach resonances in ultracold gases for two simple models and have shown the major physical result - the scattering length is a widely tunable function of an applied magnetic field. The scattering length dependence on the magnetic field has been observed experimentally and agrees with our derived results. Feshbach resonances have been crucial to the field of ultracold Fermi gases. Because of the Pauli exclusion principle, fermions tend to stay away from each other in space, but by tuning a magnetic field near a Feshbach resonance, we can cause them to interact more strongly than they would otherwise. Important recent developments like fermionic superfluidity and molecular Bose-Einstein condensates (where two fermions make the molecule) were only realized by using a magnetic field to tune the fermion-fermion interaction. Experimetnal control over the scattering length is a very powerful tool.

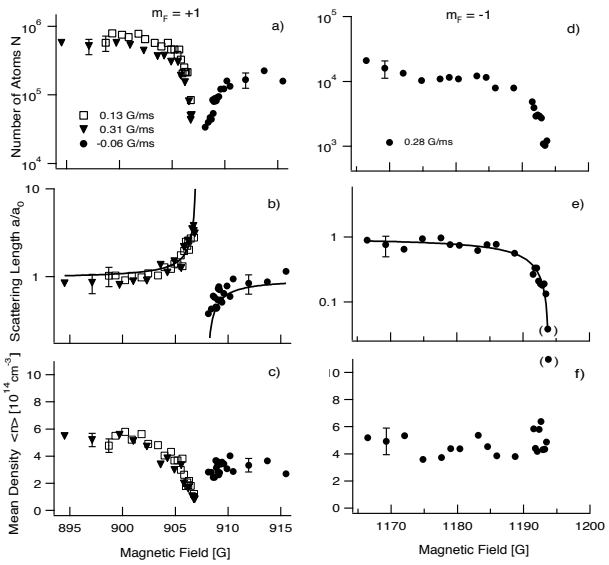

FIG. 4: Number of atoms, normalized scattering length and mean density as a function of magnetic field around the 907 G (left) and 1195 G (right) Feshbach resonances in a Bose-Einstein condensate of Na. From [13]

Acknowledgments

Thank you to Martin Zwierlein for pointing me to helpful references, and to everyone else in the Center for Ultracold Atoms.

[1] H. Feshbach, Annals of Physics (1958).
[2] W. Ketterle and M. Zwierlein, in *Proceedings of the International School of Physics "Enrico Fermi", Course CLXIV* (2006).
[3] R. L. Liboff, *Introductory Quantum Mechanics* (Addison Wesley, San Francisco, 2003), 4th ed.
[4] D. Griffiths, *Introduction to Quantum Mechanics* (Prentice Hall, Upper Saddle River, 1987), 2nd ed.
[5] D. Bohm, *Quantum Theory* (Prentice Hall, N.J., 1951).
[6] R. A. Duine and H. T. C. Stoof (2008).
[7] J. J. Sakurai, *Modern Quantum Mechanics* (Addison-Wesley, Reading, 1994).
[8] B. A. Lippmann and J. Schwinger, Physical Review **79** (1950).
[9] W. D. Phillips, in *Proceedings of the International School of Physics "Enrico Fermi"* (1992).
[10] M. W. Zwierlein, Ph.D. thesis, MIT (2006).
[11] A. J. Moerdijk, B. J. Verhaar, and A. Axelsson, Physical Review A (1995).
[12] S. Inouye, M. R. Andrews, J. Stenger, H. J. Miesner, D. M. Stamper-Kurn, and W. Ketterle, Nature **392** (1998).
[13] J. Stenger, S. Inouye, M. Andrews, H. Miesner, D. Stamper-Kurn, and W. Ketterle, Physical Review Letters (1999).
[14] G. Baym and C. J. Pethick, Physical Review Letters **76** (1996).